Sugar and Salt Concentration Detection in Water Employing ENZ Metamaterial Microwave Sensor

Shaza El-Nady
Electronics Research Institute
Asmaa Afifi
Electronics Research Institute
Anwer Ahmed (anwer.sayed@ejust.edu.eg)
Electronics Research Institute https://orcid.org/0000-0001-8636-8815

Research Article

Keywords: Antenna aperture, ENZ metamaterial, time domain, UWB, Vivaldi antenna

Posted Date: June 6th, 2022

DOI: https://doi.org/10.21203/rs.3.rs-1631463/v1

Sugar and Salt Concentration Detection in Water Employing ENZ Metamaterial Microwave Sensor

Shaza El-Nady[1], Asmaa Afifi[1], Anwer S. Abd El-Hameed[1,2]
[1] Electronics Research Institute (ERI), Giza, Egypt,
[2]Tohoku University, Center for Northeast Asian Studies, Sendai, Japan
Tel: +201224633304, +201060643078, +201061366197,
Email: shazaelnady@eri.sci.eg, anwer.sayed@eri.sci.eg

Abstract – *A design of high sensitivity Vivaldi antenna is introduced for detecting the low sugar and salt concentrations in water. The reason for selecting the Vivaldi antenna configuration is to provide two desired features; ultra-wideband and a high directivity so the surrounding clutter effect can be minimized. The prospective antenna embraces the ultra-wideband (UWB) from 4 GHz to 11 GHz. Two techniques are exploited to improve the antenna detectability; epsilon-near-zero (ENZ) metamaterial and antenna aperture amending. The ENZ metamaterial is very sensitive to the permittivity of the substrate, so any loading effect can easily alter the electric field distribution and hence affect the antenna phase properties. The high sensitivity can be increased by operating at a higher frequency. The aperture amending is used to improve substrate-air matching. An equivalent circuit model is scrutinized for further emphasis of the ENZ metamaterial operation, showing good agreement with EM simulation results. In terms of phase variation, the designed antenna is employed to sense sugar and salt in water. The amount of sugar and salt affects the material characteristics of the solution and, as a result, the reflected phases. Practical observations reveal that when the sugar and salt contents in the liquid increase, the phase falls. The simulation and measurement results of a fabricated prototype have good agreement. The time-domain analysis is discussed, revealing low distortion of received pulses.*

Keywords: *Antenna aperture, ENZ metamaterial, time domain, UWB, Vivaldi antenna*

Introduction

Water has a significant influence on the evolution of civilization. Researchers are increasingly concerned about the protection of human health. The pH factor is a critical metric to monitor in many biochemical sectors, such as food, cosmetics, and drinks. The number of diseases and deaths caused by a shortage of clean water is increasing every day [1]. Water quality is determined by a number of factors, including pH and conductivity [2, 3]. Depending on the application, pH and conductivity have a permissible limit. In [4], the existing standard approaches for designing several types of pH detectors are exhibited. The solid-state reference electrode (SSRE) is a widely used pH detector that eliminates the difficulties that plague traditional reference electrodes [5].

Drinks and food involving excessive sugar and salt have caused ailments such as diabetes, stroke, and renal failure in humans. By evaluating the material characteristics and dielectric behavior of food ingredients, a number of ideas and instruments for food evaluation have been investigated. Microwave sensors have been widely explored to identify specific qualities of nourishment materials [6]. Microwave detectors are utilizing the interaction of food substances with electromagnetic signals as a function of the dielectric permittivity of the samples, resulting in frequency deviation [7]. Sensors of moisture and humidity evaluation, biosensors, and planar sensors, as well as various detectors for sensing sugar, salinity, and other qualities in nutrition products, are now widely accessible [8]. For example, [9] presents a research based on the typical drying procedure. The level of salt in the soil is calculated using this method, which involves measuring the electrical conductivity of the soil. A coaxial probe with an open-ended was employed to follow the dielectric value in a saline-starch mixture in another way [10]. These technologies have a number of drawbacks, including high costs, complexity, and a lengthy procedure. Microwave sensors are commonly employed in healthcare devices to overcome these limits because of their short response time, immediate measurement, high sensitivity, and simplicity of usage [11]. The parameters of a device are utilized to detect variations in the examined material characteristics, and these variations are seen and clarified by the sensing constraints. Antennas are generally utilized in raio communications to send and receive electromagnetic (EM) signals. Antennas, on the other hand, can be used as sensors by employing electromagnetic waves [12]. Several antennas for detecting sugar and salt solutions have been projected in the literature. Several patch antenna configurations

employing Taconic TLY-5 material were described in [13], which can detect the sugar and salt levels in water at the resonant frequency of 2.45 GHz. An antenna with a Psi-shape based on the Rogers RT/Duroid 5880 was presented as a 16 GHz identifying device [14]. In [15], a microstrip antenna sensor with crescent-shaped is designed on a FR-4 material. A defected ground structure microstrip antenna was used to detect the quantity of sugar and salt in water [16]. The above-mentioned sensors depend on the amplitude of the reflection coefficient variation to detect only the high levels of sugar and salt concentrations.

Nowadays, artificial metamaterials have recently piqued researchers' curiosity about their unique electromagnetic characteristics [17]. The ENZ is a class of metamaterials that can be created by embedding inclusions in a periodic host media. The phase velocity of propagating waves in ENZ metamaterials is highly dependent on the substrate material and unit cell arrangement. Any modification in the loading materials can have a significant impact on the metamaterial electric field distribution in this scenario. This attribute has a big impact on how antenna phase characteristics change [18].

End-fire antennas play an important role in UWB remote sensing [19 - 21]. Two end-fire sensors are documented in the state-of-art work [22, 23]. Because of their vast bandwidth, simple shape, and widespread exploit in sensing applications, the TSA Vivaldi antennas have gotten a lot of attention. Vivaldi antennas, despite their benefits, have several disadvantages, such as a skewed beam, limited directivity, and gain when compared to other antennas. Different methods were utilized to avoid these drawbacks, like the utilization of Vivaldi antenna arrays, replacement of a part of the substrate with a dielectric lens in the antenna aperture [24], and a lens at the termination of the wings [25]. However, these solutions suffer from increasing the total size.

In this paper, a combination of ENZ metamaterials and aperture amending is utilized to enhance the Vivaldi antenna phase sensitivity to act as a microwave sensor of the low percentage of sugar and salt in water. The ENZ metamaterial unit cell is constructed as a folded line printed on a dielectric slab, while the aperture is modified with a half trapezoidal shape. The designed antenna covers a bandwidth of 4 to 11 GHz with an 8 dBi average gain from 8 GHz to 11 GHz, providing a high sensitivity with good longitudinal resolution and decreasing invasion depth to sense low amounts of diverse sugar and salt liquids. Moreover, this sensor has a short performance time and simple data interpretation. No hazardous chemicals or costly tools are required for this sensor, which reduces its complexity. Furthermore, a new approach based on the phase variation is introduced to provide higher sensitivity in case of low levels of sugar and salt concentrations.

I. Antenna Design

I.1. ENZ Unit Cell Design

The ENZ metamaterial's design is presented in this section. The ENZ metamaterial is made up of periodic unit cells that are printed on a Rogers 3010 dielectric slab with a thickness $h = 1.27mm$, a relative dielectric constant $\varepsilon_r = 10.2$, and tanδ= 0.025. This material is carefully chosen for the prospective antenna to contribute to size reduction due to its higher permittivity. The unit cell is constructed with a simple folded line shape, as shown in Fig.1 (a). The space between unit cells is kept much smaller than the operating wavelength [26], [27]. To show the electrical performance of the ENZ metamaterial unit cells, HFSS simulator is used. As shown in Fig.1 (b), two PMC boundaries are placed on both sides existing in the YZ plane, two PEC are placed perpendicular to the other two parallel PMC on both sides existing in the XZ plane, and two rectangular waveguide ports are placed on both sides existing in the XY plane. Then, the ENZ metamaterial is obtained in the x-direction [28]. The equivalent constitutive parameters are calculated using the reflection and transmission coefficients as follows [29].

$$\varepsilon = \frac{n}{Z} \tag{1}$$

$$\mu = nZ \tag{2}$$

$$Z = \pm\sqrt{\frac{(1+S_{11})^2 - S_{21}^2}{(1-S_{11})^2 - S_{21}^2}} \tag{3}$$

$$n = \frac{1}{k_0 L}\{[\mathrm{Im}[\ln(A)] + 2m\pi] + j\,\mathrm{Re}[\ln(A)]\} \tag{4}$$

$$A = \frac{S_{21}}{1 - S_{21}\dfrac{Z-1}{Z+1}} \tag{5}$$

where $S_{21}$and S_{11} are the transmission and reflection coefficients, respectively, k_0 is the propagation wave number of free space, L is the unit cell length, m is an integer value of the refractive index n, Z is the impedance of wave, μ is the equivalent permeability, and ε is the equivalent permittivity. To obtain the required low refractive index, the parameter A should be close to unity, which means that S_{11} is very small and S_{21} is close to unity, as shown in Fig.2 in the frequency band of 8 to 11 GHz. In the required frequency band, a permittivity in the x-direction of less than unity is derived as shown in Fig.3. Three primary parameters, W_1, g , and L_1, can be changed to modify the properties of ENZ unit cell resonators. The unit cell dimensions are adjusted to work in the range of 8 to 11 GHz as $L = 4mm$, $W = 4.6mm$, $L_1 = 2.75mm$, $W_1 = 0.25mm$, $g = 0.35mm$.

An LC circuit model is suggested to investigate the principle of operation of ENZ metamaterial unit cell.

Keysight ADS software has been used for circuit model analysis. It should be noticed that the equivalent inductance increases by enlarging the length of the folded line through increasing L_1 , or g. As a result, the corresponding resonant frequency will be reduced. Also, the width an W_1 has effect on the corresponding inductance. As W1 increased, the corresponding inductance is decreased, and consequently, the corresponding resonance frequency increases. The obtained ADS circuit model reflection and transmission coefficients are compared with those obtained by HFSS, showing relatively good agreement as presented in Fig.2. A wide passband can be observed from 8 to 11 GHz. Notably, the results obtained from ADS are a little bit different from those obtained with the HFSS simulator. This is attributed to the ideal behavior of the passive elements used in the proposed model. The values of inductance and capacitance of an ENZ equivalent circuit are optimized as $L_1 = 2.99\,nH$, $C_1 = 102.524\,pF$, and $C_p = 0.186pF$ and used in the HFSS simulator.

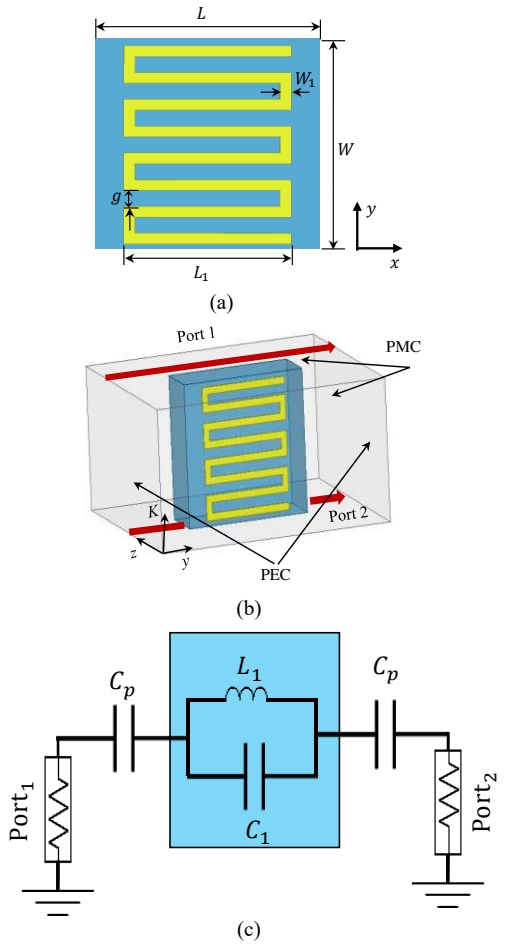

Fig.1. The proposed ENZ unit cell configuration. (a) Top view. (b) 3D- view. (c) LC circuit model.

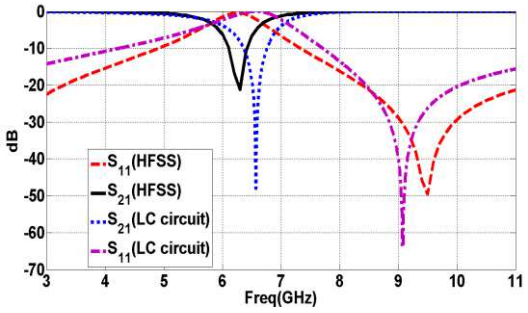

Fig.2. S-parameters of the ENZ unit cell.

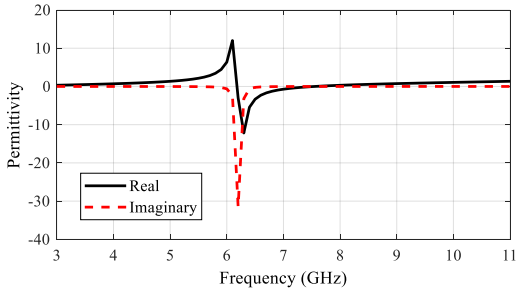

Fig.3. Retrieved effective permittivity of ENZ unit cell.

I.2. Vivaldi Antenna Design

As demonstrated in Fig. 4, the basic structure (Ant.1) is made of a pair of arms configured on opposing sides of a substrate (a). The radiated fields are created by coupling waves passing through the flared aperture inner edges. The upper arm is attached to a feeding line, and the lower arm is considered as a ground plane. A group of five unit cells of ENZ metamaterial is placed in front of the Vivaldi antenna flared aperture (Ant.2), as shown in Fig. 4 (b), to improve the antenna radiation characteristics and detectability, as will be described in the following subsection. To realize better Impedance matching between the ENZ loaded antenna and air, the substrate front-edge shape is updated to a trapezoidal shape with optimized dimensions (Ant.3), as shown in Fig.4 (c). Several simulations were run to track the influence of each alteration on the antenna operation. Fig. 5 presents the reflection coefficient of the three different cases. Good matching below -10 dB is obtained across the desired frequency range of 4 to 11 GHz. Intensive optimizations are carried out to evaluate the antenna dimensions to operate at the frequency range of 4 to 11 GHz, and they are itemized in Table I.

TABLE I
ADJUSTED DIMENSIONS OF THE VIVALDI ANTENNA IN MM

W	R_1	L	R_2	W_a	W_g	L_a	W_f	L_c	W_c
42.85	3	42.85	22.16	21.425	7.5	31.9	1.27	8.4	12.9

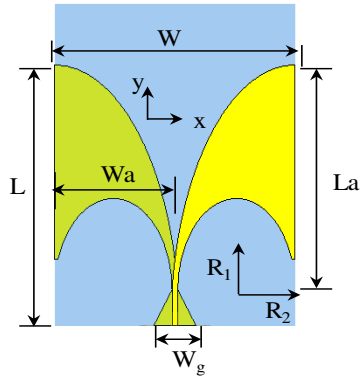

(a)

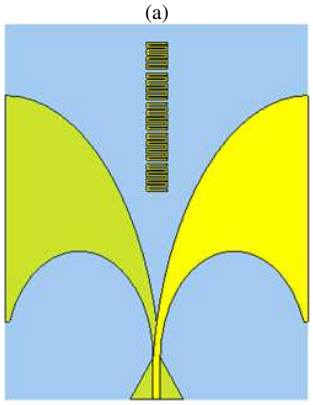

(b)

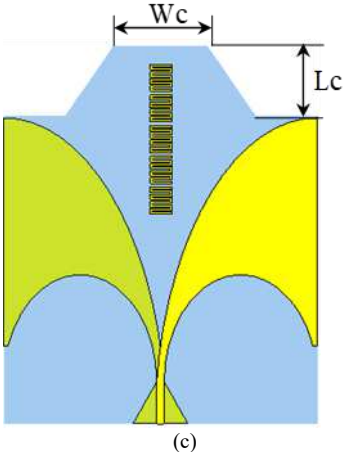

(c)

Fig. 4. Design Procedures including dimensions (a) the conventional Vivaldi antenna. (Ant.1) (b) The antenna is burdened by the ENZ unit cells (Ant.2). (c) Modified Aperture Vivaldi antenna burdened by the ENZ unit cells (Ant.3).

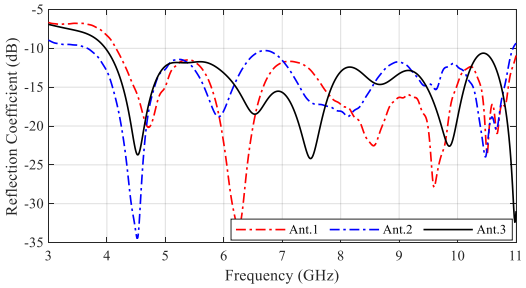

Fig. 5. The S-parameters of the design steps.

I.3. Sensitivity Improvement

The antenna sensitivity can be enhanced in the end-fire direction by adding five ENZ unit cells to the antenna aperture. In other words, by adding the ENZ unit cells, the effective permittivity is reduced in the x-direction. As a result, the propagation wave number is decreased y-direction according to the following equation [30]:

$$\frac{k_x^2}{\varepsilon_y}+\frac{k_y^2}{\varepsilon_x}=k_0^2\mu_z \qquad (6)$$

where k_x, k_y, and k_0 are the propagation constants along x, and y directions, and the free-space propagation constant. The ε_y, ε_x, and μ_z are the components of the permittivity and the permeability tensor. For the case of $\varepsilon_y \to 0$, while $\varepsilon_x \neq 0$, and $\mu_z \neq 0$, the x direction propagation constant $k_x \to 0$. Consequently, embedded ENZ unit cells in the y-direction would diminish the beamwidth in the E-plane. Subsequently, the gain and detectability of the Vivaldi antenna will be improved. In our design, the chosen number of unit cells is about to achieve the saturation level. The gain results of each design step are illustrated in Fig. 6. It is concluded that the ENZ and aperture modification significantly increases the antenna gain by about 2 dB to 4 dB in the band of 8 to 11 GHz.

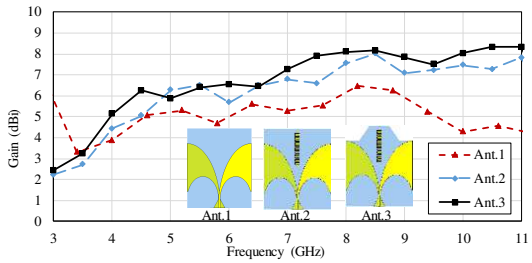

Fig. 6. Gain comparison between the antenna with and without ENZ unit cells.

II. Time Domain Analysis

The dispersion analysis of the proposed antenna can be investigated in the time domain, and a setup presented in Fig.7 is considered. This arrangement includes transmitter and receiver antennas. The transmitter antenna is placed at a certain distance, meanwhile, the receiver antenna is

interchanged circularly with angles of 0o, 45o, and 90o. The antennas are placed in the same orientation. The input signal of the Gaussian pulse is selected for the transmitter antenna to embrace the targeted UWB range [31]. As shown in Fig. 8, the antenna has a good attitude in the time domain at different angles with minimal signal degeneration, making it suitable for use in a variety of detecting systems.

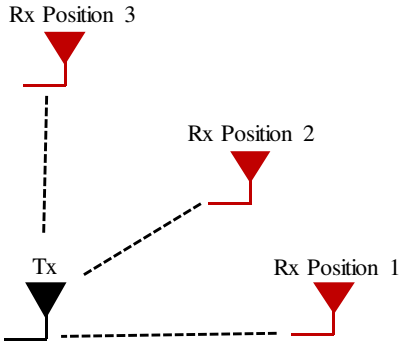

Fig. 7 Time domain evaluation setup.

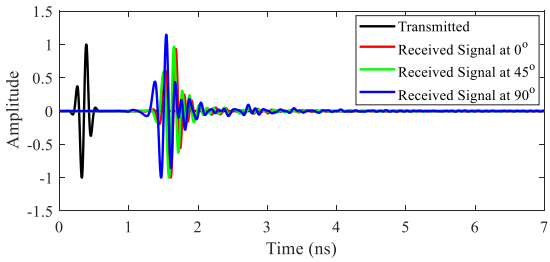

Fig. 8 Time domain signal at different angles.

III. Measurement Results and Discussion

III.1. Antenna Characteristics

Figure 9 shows the fabricated prototype with an array of ENZ unit cells. The magnitude of S_{11} was acquired using a ZVA67 Vector Network Analyzer. The measurement results of the prospective antenna is shown in Fig.10. The reflection coefficient is under -10 dB across the frequency range of 4 to 11 GHz. The end-fire gains versus frequency are plotted in Fig.11. E-plane $(x-y)$ and H-plane $(x-z)$ radiation patterns of the proposed antenna are presented at several frequencies; 8 GHz, 9.5 GHz, and 11 GHz as displayed in Fig.12, and Fig.13, respectively. It is noticed that the addition of the ENZ unit cells and the aperture reduce the beamwidth in E and H planes.

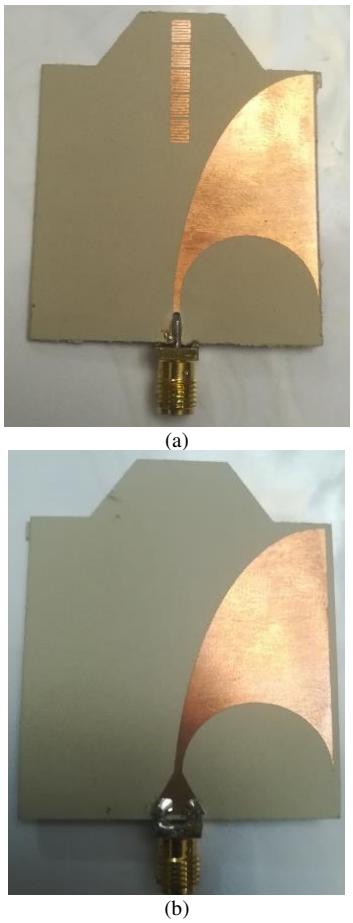

Fig. 9. Photo of the fabricated prototype (a) top view and (b) bottom view.

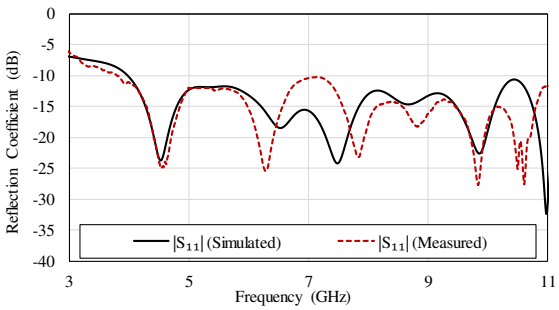

Fig. 10. S-parameters of the proposed antenna.

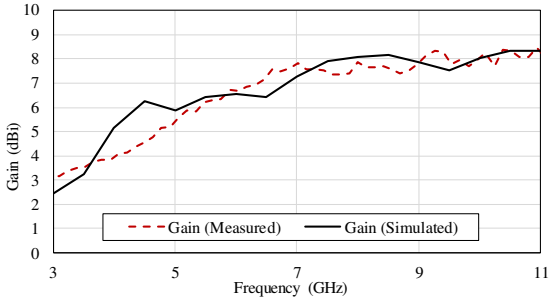

Fig. 11. Gain comparsion versus fequency.

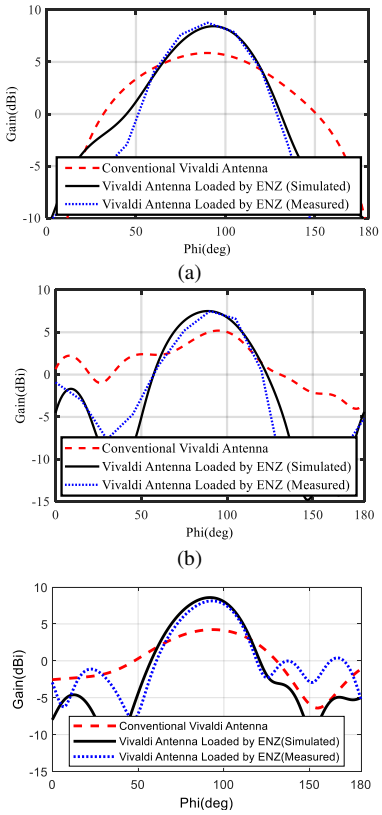

Fig. 12. Radiation patterns of the proposed antenna in the E-plane at (a) 8 GHz, (b) 9.5 GHz and (c) 11 GHz.

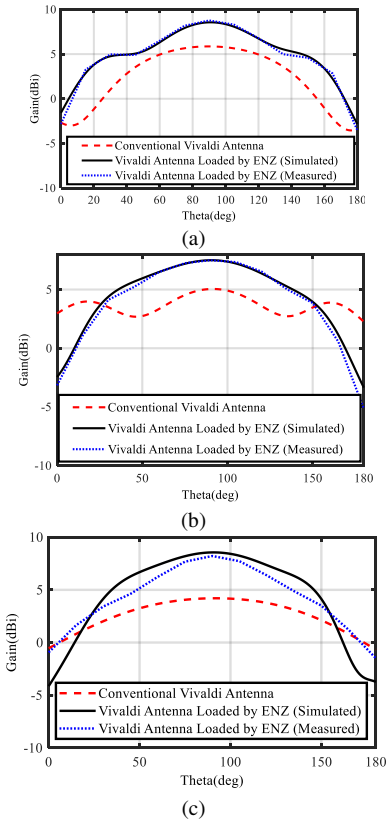

Fig. 13. Radiation patterns in the H-plane at (a) 8 GHz, (b) 9.5 GHz and (c) 11 GHz.

III.2. Sugar and Salt Concentration Detection

With increasing sugar and salt concentration liquid, the number of water molecules decreases. When sugar and salt are added to water, the water characteristics vary due to the connection between liquefied ions and water particles. Since the ionic conductivity of the solution decreases and the polarization of water decreases, the solution particles conductivity is reduced when the amount of sugar and salt increases. The decrease in ionic conductivity reduces the solution dielectric constant. Consequently, the load impedance reduces as well, resulting a reduction in phase and amplitude.

Although the change in loading material dielectric constant can be identified by the amplitude and phase of the antenna reflection coefficients. The phase is more sensitive than the amplitude in the high frequencies particularly. As a result, the authors proposed a new approach for sensing the sugar and salt concentrations based on the reflection coefficient phase. For practical examination of the offered antenna as a sensor, it is located on the water top surface as shown in Figure.14. The experiment is divided into two phases. The first part is to detect the effect of the sugar concentration, while the second part is to sense the effect of the salt concentration. The data has been acquired 10 times for different levels of concentration for both sugar and salt cases at 4 GHz, 5 GHz, 6 GHz, 7 GHz, and 8 GHz. The reflection coefficient of the antenna has been measured with the different sugar and salt concentrations using the N5227A PNA Microwave Network Analyzer at the microwave laboratory in ERI.

Fig 15 and Fig 16 present the amplitude variation of the reflection coefficient with the different percentages of sugar and salt in water respectively. It is clear that the amplitude variation is very small against the sugar and salt concentration; less than 0.05 at 5 GHz. In the high frequencies, although the amplitude variation shows higher sensitivity, in the salt case, the sugar case still needs a more accurate approach. Accordingly, we introduced the phase parameter to be an effective way for such measurements. The phase variation of reflection coefficient at the four different frequencies is investigated at 5 GHz, 6 GHz, 7GHz, and 8 GHz as illustrated in Fig 17 and Fig 18. From the results, the phase decreases obviously with a higher concentration of sugar and salt. At 5 GHz the difference between the highest and lowest sugar concentrations is about 3° in the sugar case and 5° in the salt case, but at 8 GHz, the phase difference is about 30° in the sugar case, and about 50° in the salt case. As a result, the higher frequencies are more convenient for sensing the concentration of sugar due to the shortest wavelength which provides high sensitivity.

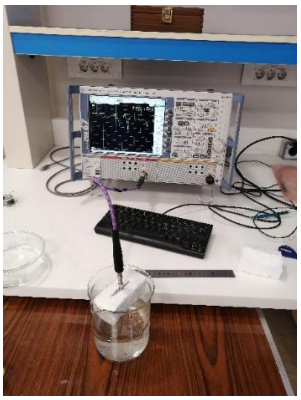

(a)

(b)

Fig. 14 Salt detection experiment setup

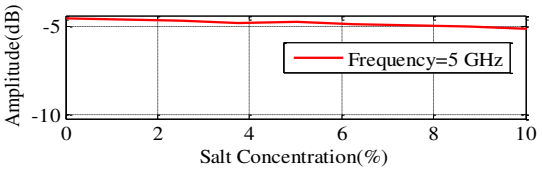

(a)

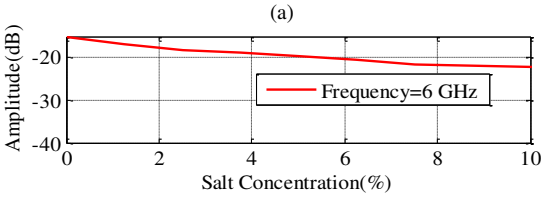

(b)

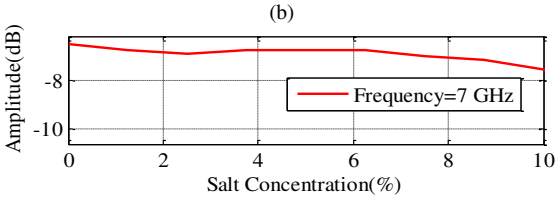

(c)

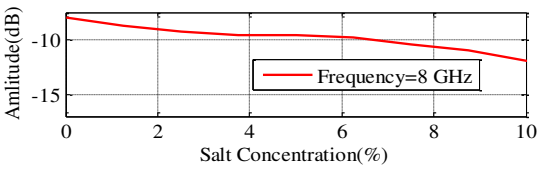

(d)

Fig. 16 Amplitude variation versus salt concentration for (a) 5 GHz (b) 6 GHz (c) 7 GHz (d) 8 GHz.

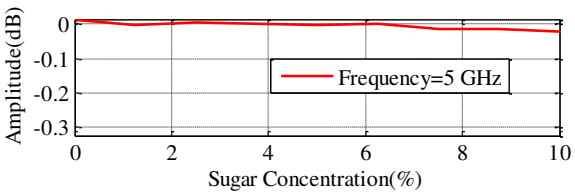

(a)

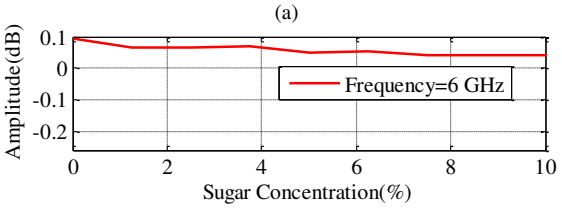

(b)

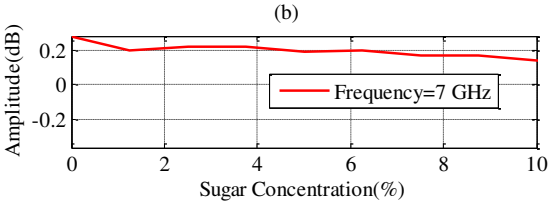

(c)

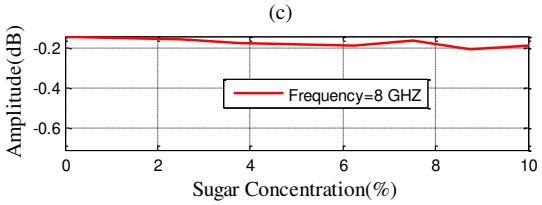

(d)

Fig. 15 Amplitude variation versus sugar concentration for (a) 5 GHz (b) 6 GHz (c) 7 GHz (d) 8 GHz

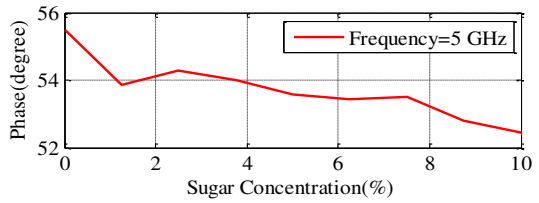

(a)

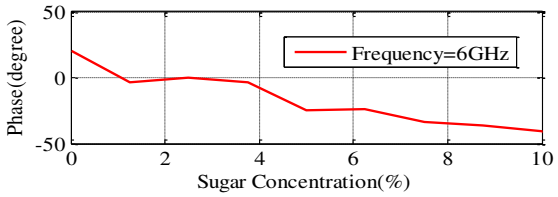

(b)

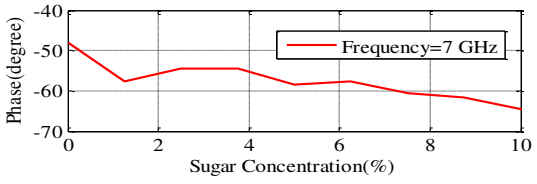

(c)

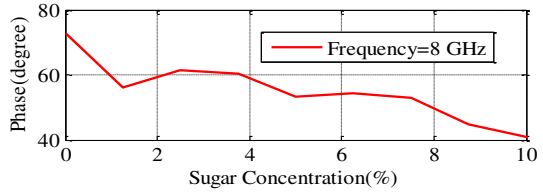

(d)

Fig. 17 Phase variation versus sugar concentration for (a) 5 GHz (b) 6 GHz (c) 7 GHz (d) 8 GHz

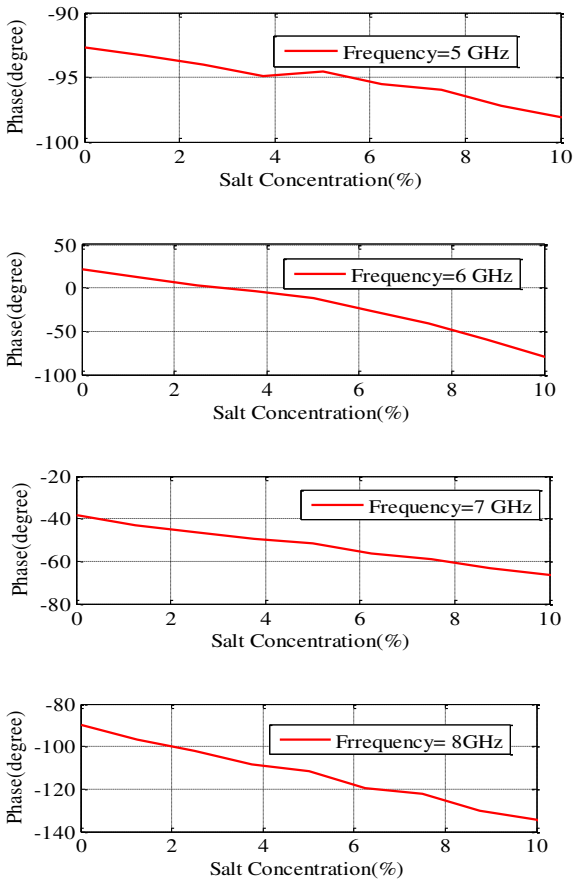

Fig. 18 Phase variation versus salt concentration for (a) 5 GHz (b) 6 GHz (c) 7 GHz (d) 8 GHz.

Table II depicts the advantage of the introduced antenna over the previous work. It is revealed that the projected antenna based on phase variation has more sensitivity at small percentages of sugar and salt. In another word, the proposed antenna can detect very low level (1%) of salt and sugar concentrations.

TABLE II
COMPARISON BETWEEN THE PROPOSED ANTENNA AND LITERATURE WORK.

Ref.	Dimensions (mm^2)	Sensor Type	Methodology	Lower limit of detection
[15]	32×22	Patch antenna	Amp. variation	20 %
[32]	50×50	Slot antenna	Amp. variation	NG
[33]	17×14	Patch antenna	Amp. variation	NG
[34]	26×24	Patch antenna	Amp. variation	10%
This work	51.3×42.9	Vivaldi antenna	Phase & amp. variation	1%

IV. Conclusion

In this paper, a high-sensitivity ENZ-based microwave sensor is presented for remote sensing applications. A reflection coefficient of less than -10 dB over the frequency band of 4 to 11 GHz is obtained. It is shown that the antenna sensitivity is improved due to increasing the gain up to 8 dBi in the frequency range of 8 GHz to 11 GHz. Simulated and measured results have good matchings. To validate the proposed microwave sensor, the reflected amplitude and phase are acquired at the top surface of the sugar and salt solution. As the percentages of sugar and salt increase, the phase and reflection coefficients decrease. However, the phase variation is much higher than the amplitude. The results reveal that the provided sensor has a high sensitivity for detecting low sugar and salt concentrations in water. Because the amount of sugar and salt in food and drink is required by law, this cheap device can be exploited in the food and drink business to sense sugar and salt percentage.

References

[1] Bertuzzo, E., & Mari, L. (2017). Hydrology, water resources and the epidemiology of water-related diseases. *Advances in Water Resources, 108, 329-331.*

[2] Afrand, M., Esfe, M. H., Abedini, E., & Teimouri, H. (2017). Predicting the effects of magnesium oxide nanoparticles and temperature on the thermal conductivity of water using artificial neural network and experimental data. *Physica E: Low-dimensional Systems and Nanostructures, 87, 242-247.*

[3] C.Zhang, H.Ye, F. Liu, Y. He, W. Kong, and K. Sheng, Determination and visualization of pH values in anaerobic digestion of water hyacinth and rice straw mixtures using hyperspectral imaging with wavelet transform denoising and variable selection, *Sensors , Volume 16,* (Issue 2), *February 2016, pages 244.*

[4] Zhang, C., Ye, H., Liu, F., He, Y., Kong, W., & Sheng, K. (2016). Determination and visualization of pH values in anaerobic digestion of water hyacinth and rice straw mixtures using hyperspectral imaging with wavelet transform denoising and variable selection. *Sensors, 16(2), 244.*

[5] Kim, T. Y., Hong, S. A., & Yang, S. (2015). A solid-state thin-film Ag/AgCl reference electrode coated with graphene oxide and its use in a pH sensor. *Sensors, 15(3), 6469-6482.*

[6] Mohammad, A. M., Chowdhury, T., Biswas, B., & Absar, N. (2018). Food poisoning and intoxication: A global leading concern for human health. *In Food safety and preservation (pp. 307-352). Academic Press.*

[7] Posudin, Y., Peiris, K., & Kays, S. (2015). Non-destructive detection of food adulteration to guarantee human health and safety.

[8] Lin, B., & Wang, S. (2020). Dielectric properties, heating rate, and heating uniformity of wheat flour with added bran associated with radio frequency treatments. *Innovative Food Science & Emerging Technologies, 60, 102290.*

[9] Gartley, K. L. (2011). Recommended methods for measuring soluble salts in soils. Recommended soil testing procedures for the northeastern United States. *Northeastern Regional Publication, 493, 1864-2.*

[10] Bircan, C., & Barringer, S. A. (1998). Salt-starch interactions as evidenced by viscosity and dielectric property measurements. *Journal of Food Science, 63(6), 983-986.*

[11] Omer, A. E., Shaker, G., Safavi-Naeini, S., Ngo, K., Shubair, R. M., Alquié, G., ... & Kokabi, H. (2020). Multiple-cell microfluidic dielectric resonator for liquid sensing applications. *IEEE Sensors Journal, 21(5), 6094-6104.*

[12] Govind, G., & Akhtar, M. J. (2019). Metamaterial-inspired microwave microfluidic sensor for glucose monitoring in aqueous solutions. *IEEE Sensors Journal, 19(24), 11900-11907.*

[13] Cheng, E. M., Fareq, M., Shahriman, A. B., Mohd Afendi, R., Lee, Y. S., Khor, S. F., ... & Jusoh, M. A. (2014). Development of

microstrip patch antenna sensing system for salinity and sugar detection in water. *Int. J. Mech. Mechatronics Eng, 15(5), 31-36.*
[14] Rahman, M. N., Islam, M. T., & Samsuzzaman Sobuz, M. (2018). Salinity and sugar detection system using microstrip patch antenna. *Microwave and Optical Technology Letters, 60(5), 1092-1096.*
[15] Islam, M. T., Rahman, M. N., Singh, M. S. J., & Samsuzzaman, M. (2018). Detection of salt and sugar contents in water on the basis of dielectric properties using microstrip antenna-based sensor. *IEEE Access, 6, 4118-4126.*
[16] Njokweni, S. N., & Kumar, P. (2020). Salt and sugar detection system using a compact microstrip patch antenna. *Int J Smart Sensing Intell Syst, 13(1), 1-9.*
[17] Devapriya, A. T., & Robinson, S. (2019). Investigation on metamaterial antenna for terahertz applications. *Journal of Microwaves, Optoelectronics and Electromagnetic Applications, 18, 377-389.*
[18] Alu, A., Silveirinha, M. G., Salandrino, A., & Engheta, N. (2007). Epsilon-near-zero metamaterials and electromagnetic sources: Tailoring the radiation phase pattern. *Physical review B, 75(15), 155410.*
[19] Sun, F., Zhang, F., & Feng, C. (2019). Wideband pattern reconfigurable printed-Yagi antenna array based on feed structure. Journal of Microwaves, Optoelectronics and *Electromagnetic Applications, 18, 270-275.*
[20] Abd El-Hameed, A. S., Mahmoud, N., Barakat, A., Abdel-Rahman, A. B., Allam, A., & Pokharel, R. K. (2016, April). A 60-GHz on-chip tapered slot Vivaldi antenna with improved radiation characteristics. In 2016 10th European Conference on Antennas and Propagation (EuCAP) (pp. 1-5). IEEE.
[21] Abd El-Hameed, A. S., Mahmoud, N., Barakat, A., Abdel-Rahman, A. B., Allam, A., & Pokharel, R. K. (2016, April). A 60-GHz on-chip tapered slot Vivaldi antenna with improved radiation characteristics. In 2016 10th European Conference on Antennas and Propagation (EuCAP) (pp. 1-5). IEEE.
[22] Molaei, A., Kaboli, M., Mirtaheri, S. A., & Abrishamian, S. (2014, January). Beam-tilting improvement of balanced antipodal vivaldi antenna using a dielectric lens. In Proc. 2nd Iranian Conference on Engineering Electromagnetics (pp. 577-581).
[23] Fei, P., Jiao, Y. C., Hu, W., & Zhang, F. S. (2011). A miniaturized antipodal Vivaldi antenna with improved radiation characteristics. *IEEE antennas and wireless propagation letters, 10, 127-130.*
[24] Amiri, M., Tofigh, F., Ghafoorzadeh-Yazdi, A., & Abolhasan, M. (2017). Exponential antipodal Vivaldi antenna with exponential dielectric lens. *IEEE Antennas and Wireless Propagation Letters, 16, 1792-1795.*
[25] Teni, G., Zhang, N., Qiu, J., & Zhang, P. (2013). Research on a novel miniaturized antipodal Vivaldi antenna with improved radiation. *IEEE Antennas and Wireless Propagation Letters, 12, 417-420.*
[26] Popescu, A. S., Bendoym, I., Rexhepi, T., & Crouse, D. (2016). Anisotropic zero index material: A method of reducing the footprint of Vivaldi antennas in the UHF range. *Progress In Electromagnetics Research C, 65, 33-43.*
[27] Tang, W. X., Zhao, H., Zhou, X., Chin, J. Y., & Cui, T. J. (2008). Negative index material composed of meander line and SRRs. *Progress In Electromagnetics Research, 8, 103-114.*
[28] Bhaskar, M., Johari, E., Akhter, Z., & Akhtar, M. J. (2016). Gain enhancement of the Vivaldi antenna with band notch characteristics using zero-index metamaterial. *Microwave and Optical Technology Letters, 58(1), 233-238.*
[29] Smith, D. R., Schultz, S., Markoš, P., & Soukoulis, C. M. (2002). Determination of effective permittivity and permeability of metamaterials from reflection and transmission coefficients. *Physical review B, 65(19), 195104.*
[30] Zhou, B., Li, H., Zou, X., & Cui, T. J. (2011). Broadband and high-gain planar Vivaldi antennas based on inhomogeneous anisotropic zero-index metamaterials. *Progress In Electromagnetics Research, 120, 235-247.*
[31] Abd El-Hameed, A. S., Wahab, M. G., Elboushi, A., & Elpeltagy, M. S. (2019). Miniaturized triple band-notched quasi-self complementary fractal antenna with improved characteristics for UWB applications. *AEU-international journal of electronics and communications, 108, 163-171.*
[32] Jain, S. (2022). Early Detection of Salt and Sugar by Microstrip Moisture Sensor Based on Direct Transmission Method. *Wireless Personal Communications, 122(1), 593-601.*
[33] Kaur, J., & Khanna, R. (2022). Novel monkey-wrench-shaped microstrip patch sensor for food evaluation and analysis. *Journal of the Science of Food and Agriculture, 102(4), 1443-1456.*
[34] Rahman, M. N., Hassan, S. A., Samsuzzaman, M., Singh, M. S. J., & Islam, M. T. (2019). *Determination of salinity and sugar concentration using microwave sensor. Microwave and Optical Technology Letters, 61(2), 361-364.*

Data and Code Availability Statement

Data and code sharing is not applicable to this article.

Funding Declaration

The authors declare that no funds, grants, or other support were received during the preparation of this manuscript.

Conflicts of Interests

The author(s) declares that there is no conflicts of interest with respect to the research, authorship, and/or publication of this paper anywhere.

Authors Contribution

All authors contributed to the study conception. Design and simulation were performed by [Shaza El-Nady], [Asmaa Afifi]. Data collection and analysis were performed by all authors. The first draft of the manuscript was written by [Shaza El-Nady] and [Anwer S. Abd El-Hameed] all authors commented on previous versions of the manuscript. All authors read and approved the final manuscript.

Shaza M. Elnady received the B.Sc. degree in Electronics and Communications Engineering from the Faculty of Engineering, Benha University, Egypt, in 2003, the M.Sc. degree in electronics and communication engineering from Al-Azhar University, Egypt, in 2012, and Ph.D. degree in Electronics and Communication Engineering from Ain-Shams University, Egypt, in 2019. She works as a researcher at the Electronics Research Institute, Egypt. Her research interests include mm-wave circuits, microstrip circuits, metamaterial, and microwave imaging.

Asmaa I. Afifi received the B.S. degree in electrical engineering from Al-Azhar University Egypt, in 2012, M.S. and PhD. degree in electronics and communications engineering from the Egypt-Japan University of Science and Technology (E-JUST), Alexandria, Egypt, in 2017 and 2021. From 2013 to 2017, she was a Research Assistant, then, she promoted to Assistant Researcher from 2013 to 2021 at the Microstrip Circuits Department, Electronics Research Institute, Egypt. She is currently Researcher with the Electronics Research Institute Her research interests include planar antennas, DRA antennas, MIMO antennas, and sensors design for breast cancer detection.

Anwer S. Abd El-Hameed (Member, IEEE) received the B.Sc. degree in electronics and communication engineering from Al-Azhar University, Egypt, in 2009, the M.Sc. degree in electronics and communication engineering from Cairo University, Egypt, in 2014, and the Ph.D. degree from the Egypt-Japan University of Science and Technology, Egypt, in May 2018. He has been working with the Microstrip Circuits Department, Electronics Research Institute, Cairo, Egypt, since 2010 (on leave). He joined Kyushu University, Fukuoka, Japan, as a Special Research Student, as a part of his Ph.D. program, in June 2017. He has been a Postdoctoral Research Fellow with the Center for Northeast Asian Studies, Tohoku University, Sendai, Japan, since January 2019. He is currently an assistant professor at Tohoku University. His research interests include planar antennas, on-chip antennas, mm-wave circuits, WPT, metamaterials, microwave imaging, archeological survey based on electromagnetic waves, and developing radar systems for cultural heritage preservation and ground surface disaster prevention. He is a Guest Editor of the Special Issue of Microwave Subsystems and Wireless Propagation in the journal of Electronics (MDPI).